

Three-Dimensional Characteristics of Diurnally Varying Boundary-Layer Flows

JAN PAEGLE and GLENN E. RASCH—*Department of Meteorology,
The University of Utah, Salt Lake City, Utah*

ABSTRACT—Numerical models of three-dimensional, diurnally varying, boundary-layer flows are integrated to study the effect of fluctuating pressure gradients and eddy stresses within different circulation systems. The computational problem is reduced by expanding the horizontal dependence of solutions into Taylor series truncated at the first two terms. Within this simplification, sufficient generality is retained to reproduce axially symmetric similarity solutions and solutions of the nonlinear balance

equation. For the time-dependent cases, substantial deviations from linearized (horizontally uniform) theory are predicted. Diurnally periodic pressure gradient and eddy stress oscillations cause greatly differing responses for various circulation systems. The magnitude of the balanced vorticity and the nature of the local deformation field have great bearing on the development of boundary-layer jets and secondary vertical circulations.

1. INTRODUCTION

Large day-to-night variations of planetary boundary-layer winds are observed in many parts of the world. An illustration is given in the time section of wind speeds at Fort Worth, Tex., displayed in figure 1. This analysis (taken from pibal wind data at 6-hr intervals) shows a prominent wind oscillation, with greatest amplitude around 500 m. The diurnal rotation of the vector wind is shown in figure 2.

This example is typical of summer conditions over the Great Plains, and larger wind oscillations are often observed north of Fort Worth (Bonner 1965). Similar oscillations occur over England and France (Kendrew 1957), Eastern Europe (Novozhilov 1961), Africa (Farquharson 1939), Australia (Allen 1971), and Argentina (Altinger 1972).

Strong nocturnal jets, several hundred meters above the ground, usually accompany the oscillation. In some locations, these jets appear to be related to high frequencies of nocturnal thunderstorms. These aspects are best documented over the Great Plains of the United States. (see, for example, Blackadar 1957, Pitchford and London 1962, Bonner and Paegle 1970.) Bonner et al. (1968) report 500-m wind speeds 70 percent above geostrophic and kinematically computed vertical velocities on the order of 1 cm/s in an average of 10 Great Plains nocturnal jet cases.

It is quite clear that the wind oscillation is forced by diurnal oscillations of eddy stress and buoyancy forces above sloping terrain. The former effect has been modeled by Ooyama (1957), Buajitti and Blackadar (1957), and Krishna (1968), and the latter by Holton (1967). The combined effect has been modeled by Bonner and Paegle (1970). Most of these models predict winds barely 30 percent larger than geostrophic, and all exclude horizontal flow variation, thereby ignoring boundary-layer induced

vertical velocities. Thus, while such models do explain qualitative features of the diurnal wind oscillations, they do not explain the very large nocturnal jets, and they have ignored altogether their possible connection with diurnal oscillations of vertical motions and related weather.

The simplifying assumption of horizontal flow uniformity is justified by scale analysis for flows such that the Rossby number,

$$Ro = \frac{|\nabla|\mathbf{V}||}{f},$$

(where $|\nabla|\mathbf{V}||$ is the horizontal wind speed gradient and f is the Coriolis parameter) is much smaller than one. The case studies of Bonner et al. (1968) reveal flow gradients close to $f/2$ and imply $Ro = 1/2$. It is not correct to omit horizontal flow variation in the equations of motion when modeling such cases.

It is the purpose of this investigation to model the effect of the nonlinear terms arising from the horizontal variation of the horizontal pressure gradient. It will be shown that moderate Rossby number flows can be substantially different from $Ro = 0$ flows for diurnally forced motion. A principal reason is that the natural period of oscillation on the rotating earth is $2\pi/(f + \xi)$, where ξ is the relative vorticity. A diurnal forcing is resonant with this at different critical latitudes, and the magnitude of the response of the wind is a sensitive function of ξ .

In sections 2 and 3, the main effects of diurnal eddy stress oscillation and of pressure gradient oscillation are outlined for horizontally uniform flow and height-constant eddy viscosity. This facilitates interpretation of results of section 4, where horizontal flow variations are retained in two simplified numerical approaches. Solutions are expressed as truncated series expansions in Ro in one approach and as truncated series expansions in x and y in the other. The latter approach is more flexible and is

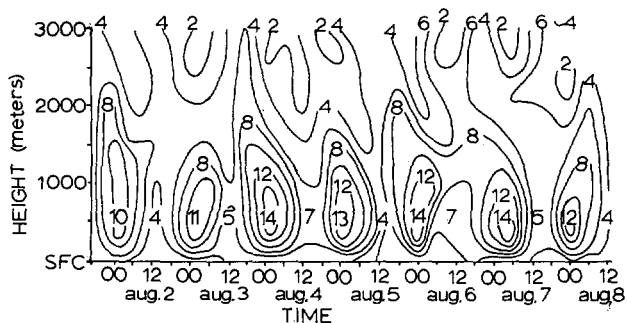


FIGURE 1.—Time section of wind speeds (m/s) at Fort Worth, Tex., for Aug. 2-8, 1960.

used to model boundary-layer flows over flat and curved terrain, and with constant and variable Coriolis parameter. In either approach, the numerical problem reduces to time integrations of parabolic diffusion-type equations in the single space dimension, z .

2. EFFECT OF EDDY STRESS OSCILLATION

Turbulent transfer of momentum through the planetary boundary layer to the ground tends to be much greater during the afternoon of a sunny day than during the night. Consequently, afternoon winds usually have ageostrophic components directed toward low pressure. As the thermally induced turbulence diminishes around sunset, the downward momentum transfer becomes negligible, and the ageostrophic component of the afternoon begins to rotate in an inertial oscillation. When it aligns with the geostrophic wind vector around midnight, a supergeostrophic flow is observed. This is the basis of models simulating the nocturnal jet through eddy stress oscillation.

The simplest time-dependent mathematical model of this process assumes horizontal homogeneity and formulates eddy stresses in terms of a height invariant eddy viscosity. The momentum equation governing the motion is

$$\frac{\partial(u+iv)}{\partial t} + if(u+iv) = if(u_g + iv_g) + K \frac{\partial^2(u+iv)}{\partial z^2}. \quad (1)$$

Here, (u, v) and (u_g, v_g) are eastward and northward components of the wind and geostrophic wind, respectively, t is time, z is height, and K is the eddy viscosity. The diurnal eddy stress oscillation may be modeled by

$$K = A(1 - \nu \cos \Omega t) \quad (2)$$

where Ω is the diurnal frequency. Two approaches for the solution of this problem are outlined by Ooyama (1957) and Paegle (1970). The periodic solution is

$$u+iv = (u_g + iv_g) \left\{ 1 - \sum_{n=-\infty}^{\infty} A_n \exp \left[- \left(\frac{i\omega_n f}{A} \right)^{1/2} z - i\omega_n \frac{\nu f}{\Omega} \sin \Omega t \right] \right\} \quad (3)$$

where

$$\omega_n = \frac{n\Omega + f}{f}, \quad (4)$$

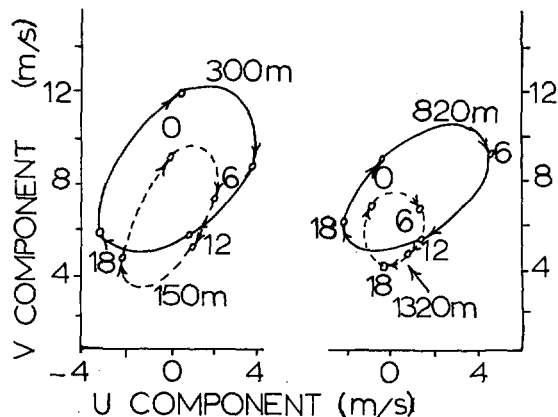


FIGURE 2.—Mean wind oscillation (m/s) at various levels for Aug. 2-8, 1960, at Fort Worth. Times are csr.

$$A_n = \frac{f}{n\Omega + f} J_n \left(\nu \frac{n\Omega + f}{\Omega} \right), \quad (5)$$

$$(i)^{1/2} = \frac{1+i}{\sqrt{2}}, \quad (-i)^{1/2} = \frac{1-i}{\sqrt{2}}. \quad (6)$$

J_n is a Bessel function of order n .

A_n and ω_n are functions of latitude and determine the response of the flow oscillation for given ν . At the level of the model nocturnal jet, the most important contribution to solution (3) is from the lowest mode ($n = -1$), and this is maximum at 30° latitude where

$$\omega_{-1} = 0 \text{ and } A_{-1} = \frac{\nu}{2}.$$

Thus at 30° latitude, the wind can be almost 50 percent supergeostrophic at the time of minimum eddy viscosity. The magnitude of the oscillation diminishes with distance from 30° , and only a 30-percent supergeostrophic component is predicted at 40° .

Qualitatively, similar results are obtained for the K variable in height (Ooyama 1957) for discontinuous variation of K from day to night (Paegle 1970) and in more complete numerical investigations (Krishna 1968). The strongest response is predicted for 30° latitude, and it weakens toward the middle latitudes where the strongest jets are observed. Thus, the eddy stress fluctuation is apparently insufficient to explain the strong nocturnal jets observed over the Great Plains.

3. EFFECT OF PRESSURE GRADIENT OSCILLATION

The daily temperature cycle over sloping terrain produces important pressure gradient oscillations, even over terrain slopes as gentle as those of the Great Plains (1/500). Day-to-night variations of the associated geostrophic wind field amount to about 6-8 m/s (Sangster 1967, Bonner and Paegle 1970).

The most complete model of the effect of this on boundary-layer flow is given by Holton (1967). A simplified version indicates some of the important features of the solution. The solution to eq (1) with geostrophic wind,

$$V_g = (\bar{u}_g + i\bar{v}_g) + i\Delta V e^{-z/H} \cos \Omega t, \quad (7)$$

is

$$(u + iv) = (\bar{u}_g + i\bar{v}_g) [1 - e^{-(1+i)z\sqrt{f/2K}}]$$

$$\begin{aligned} & - \left[\frac{e^{-i\Omega t}}{2 \left[\frac{K}{H^2} + i(\Omega - f) \right]} - \frac{e^{i\Omega t}}{2 \left[-\frac{K}{H^2} + i(\Omega + f) \right]} \right] f \Delta V e^{-z/H} \\ & - \underbrace{\left[\frac{-e^{-i\Omega t} e^{-(1+i)\sqrt{\frac{f-\Omega}{2K}}z}}{2 \left[\frac{K}{H^2} + i(\Omega - f) \right]} + \frac{e^{+i\Omega t} e^{-(1+i)\sqrt{\frac{f+\Omega}{2K}}z}}{2 \left[-\frac{K}{H^2} + i(\Omega + f) \right]} \right]}_* f \Delta V \end{aligned}$$

for $f > \Omega$ (poleward of 30°N).

$$* \text{ term} \rightarrow \frac{-e^{-i\Omega t} H^2}{2K} \quad \text{for } f \rightarrow \Omega \text{ (30°N lat.)} \quad (8)$$

and

$$\frac{-e^{-i\Omega t} e^{-(1+i)\sqrt{\frac{\Omega-f}{2K}}z}}{2 \left[\frac{K}{H^2} + i(\Omega - f) \right]} \quad \text{for } f < \Omega \text{ (south of 30°N).}$$

The first bracket of the solution is the Ekman spiral for the mean geostrophic wind. The second bracket is a diurnally periodic expression damping in height in the same manner as the forcing. The third bracket is also a diurnally periodic term and represents most of the response for f close to Ω (close to 30° latitude). The strongest response exists at the critical latitude of 30°, and here the solution is very sensitive to the value of H . The observed Great Plains pressure oscillation is well modeled by eq (7) when H is about 800 m and ΔV is about 3 to 4 m/s (Bonner and Paegle 1970), and an appropriate magnitude for K is probably on the order of 10 m²/s. Thus, nocturnal jets about 8 m/s above geostrophic may be anticipated at 30°, and this model could easily explain observations in the immediate vicinity of 30°. However, the response drops sharply at relatively small distances from this latitude, and the model is not adequate over most of the Great Plains.

Bonner and Paegle (1970) combined the effects of eddy stress oscillation and pressure gradient oscillation in quadrature evaluations of integral solutions of eq (1). The amplitude of the simulated wind oscillation was close to that observed in an average of 9 yr of summer rawinsonde data at Fort Worth, when the diurnal pressure fluctuation was specified to match local topographic influences. However, the amplitude of the model remains less than that observed in strong instances, and the nocturnal speed predicted by the model diminishes at more northerly latitudes instead of increasing as observed.

From the above, it may be concluded that:

1. Models for diurnal boundary-layer wind oscillation show a marked amplification at the critical latitude of 30°.
2. Current models underestimate the nocturnal jet, except in the immediate vicinity of 30°.

It follows that an important effect is not adequately modeled in the above-mentioned references.

Among the simplifying assumptions of the analyses of sections 1 and 2, those with greatest implication are probably:

1. Atmospheric stratification is neglected.
2. Horizontally uniform flow is assumed.
3. The eddy viscosity is unrealistic, especially at low levels where K is maintained constant in height.

Holton (1967) has shown that stable stratification tends to decrease the wind oscillation. For unstable conditions, a much smaller horizontal scale than that of the observed nocturnal jet would be predicted. A realistic inclusion of stratification would greatly complicate the analysis. Except for the diurnal variation of the momentum exchange coefficient, neutral conditions will be assumed. Assumptions 2 and 3 will be relaxed in the next section.

4. EFFECT OF HORIZONTAL VARIATION

The phenomenon of resonance at a critical latitude is modified if the atmosphere has nonzero vorticity, ξ , relative to the earth. The critical latitude of maximum response is then no longer 30°, but whichever latitude is such that $\xi + f = 2\pi/(1 \text{ day})$ (if it exists). A straightforward application of the analysis of the previous sections, replacing f with absolute vorticity, is not possible because in the boundary layer the relative vorticity also fluctuates from day to night and the problem is nonlinear. A three-dimensional model incorporating horizontal variation is needed.

Numerical integration of such a model can become prohibitively expensive unless simplifications are introduced. In this paper, the horizontal space dependence of the flow is specified analytically to reduce the computational effort, and the time and height dependence of this specified horizontal variation is forecast numerically.

For incompressible flow, the relevant equations are

$$\frac{\partial u}{\partial t} + u \frac{\partial u}{\partial x} + v \frac{\partial u}{\partial y} + w \frac{\partial u}{\partial z} - fv = -fv_g + \frac{\partial}{\partial z} \left(K \frac{\partial u}{\partial z} \right), \quad (9)$$

$$\frac{\partial v}{\partial t} + u \frac{\partial v}{\partial x} + v \frac{\partial v}{\partial y} + w \frac{\partial v}{\partial z} + fu = fu_g + \frac{\partial}{\partial z} \left(K \frac{\partial v}{\partial z} \right), \quad (10)$$

and

$$\frac{\partial w}{\partial z} + \frac{\partial u}{\partial x} + \frac{\partial v}{\partial y} = 0. \quad (11)$$

The velocity components at any point (x, y) can be expanded into a Taylor series about (x_0, y_0) . Assuming flow fields such that second and higher order derivatives are negligible and translating the origin to (x_0, y_0) , we get

$$u = U + u_x x + u_y y, \quad (12)$$

$$v = V + v_x x + v_y y, \quad (13)$$

and

$$w = W, \quad (14)$$

where

$$U = u(x=0, y=0, z, t), \quad (15)$$

$$V = v(x=0, y=0, z, t), \quad (16)$$

$$\left(\frac{\partial}{\partial x} \right) \Big|_{x=y=0}, \quad (17)$$

and

$$\left(\frac{\partial}{\partial y} \right) \Big|_{x=y=0}. \quad (18)$$

For the assumed horizontal variation of u and v , continuity requires horizontally uniform w . Substituting the above expansion into the equations of motion, noting that coefficients of x and y must vanish identically in each equation, and maintaining K horizontally uniform, we obtain

$$\frac{\partial U}{\partial t} + Uu_x + Vu_y + W \frac{\partial U}{\partial z} - f_0 V = -f_0 v_g + \frac{\partial}{\partial z} \left(K \frac{\partial U}{\partial z} \right), \quad (19)$$

$$\frac{\partial V}{\partial t} + Uv_x + Vv_y + W \frac{\partial V}{\partial z} + f_0 U = f_0 u_g + \frac{\partial}{\partial z} \left(K \frac{\partial V}{\partial z} \right), \quad (20)$$

$$\frac{\partial u_x}{\partial t} + u_x u_x + v_x u_y + W \frac{\partial u_x}{\partial z} - f_0 v_x = -f_0 v_{gx} + \frac{\partial}{\partial z} \left(K \frac{\partial u_x}{\partial z} \right), \quad (21)$$

$$\frac{\partial v_x}{\partial t} + u_x v_x + v_x v_y + W \frac{\partial v_x}{\partial z} + f_0 u_x = f_0 u_{gx} + \frac{\partial}{\partial z} \left(K \frac{\partial v_x}{\partial z} \right), \quad (22)$$

$$\frac{\partial u_y}{\partial t} + u_y u_x + v_y u_y + W \frac{\partial u_y}{\partial z} - f_0 v_y - \beta V = -f_0 v_{gy} + \frac{\partial}{\partial z} \left(K \frac{\partial u_y}{\partial z} \right), \quad (23)$$

and

$$\frac{\partial v_y}{\partial t} + u_y v_x + v_y v_y + W \frac{\partial v_y}{\partial z} + f_0 u_y + \beta U = f_0 u_{gy} + \frac{\partial}{\partial z} \left(K \frac{\partial v_y}{\partial z} \right), \quad (24)$$

$$\frac{\partial W}{\partial z} + u_x + v_y = 0. \quad (25)$$

In these equations, u_g , v_g , u_{gx} , v_{gx} , u_{gy} , v_{gy} denote geostrophic winds and their lateral gradients, and f_0 and β are constant midlatitude values of f and df/dy . Benton et al. (1964) investigated a similar system for steady state with $\beta=0$ and $K=\text{constant}$.

Although highly simplified, the equations retain sufficient generality to reproduce several flows of interest in meteorology. For purely rotational, frictionless, steady flows with $\beta=0$, the solutions give the gradient wind. In the limiting case of circular vortices with $\beta=0$, the assumed space dependence is that of the similarity solutions (e.g., Greenspan 1968, pp. 133-141), and the equations are equivalent in that case. Adding eq (23) and (24), we obtain a divergence equation for which the solution in the steady-state frictionless limit is just the same as that of

the nonlinear balance equation with appropriate boundary conditions.

An important limitation is that higher order horizontal derivatives of the flow field are neglected. In particular, the system of equations would be inadequate in regions of strong relative vorticity advection. Since for many midlatitude situations the relative vorticity advection is of the same order as the β effect, it will be possible to assess some measure of this simplification by comparing results of experiments that include and drop β , and which are otherwise identical.

Numerical Methods

In numerical integration, boundary conditions must be imposed at the upper and lower limits of integration. At the lower boundary (the roughness height), the boundary conditions specify zero flow. At the top boundary (located close to 2000 m in all experiments), two boundary conditions were tested. The no-stress boundary condition,

$$\left[\frac{\partial(\quad)}{\partial z} = 0 \right], \quad (26)$$

works well for flows with small deformation; that is, $(\partial u/\partial y + \partial v/\partial x)$ and $(\partial u/\partial x - \partial v/\partial y)$ are small relative to f , but proves slightly unstable in the presence of significant deformation. The upper boundary condition used in the experiments to be shown is the solution to the balance equation. For the case that $\beta=0$, this can be obtained explicitly from the above equations by specifying $K=0$, $\partial(\quad)/\partial z=0$, and $\partial/\partial t=0$. Then

$$U = \frac{-f_0[v_g v_y + u_g(u_y - f)]}{(v_x + f_0)(f_0 - u_y) + u_x v_y} \quad (27)$$

and

$$V = \frac{-v_g(v_x + f_0)f_0 - u_g f_0 u_x}{(u_y - f_0)(v_x + f_0) - u_x v_y} \quad (28)$$

with

$$u_x = u_{gx} = -v_y = -v_{gy}, \quad (29)$$

$$u_y = \frac{(v_{gx} + u_{gy} + f_0) - [(u_{gy} + v_{gx} + f_0)^2 - 4f_0 u_{gy} + 4u_{gx}^2]^{1/2}}{2}, \quad (30)$$

and

$$v_x = v_{gx} + u_{gy} - u_y. \quad (31)$$

For nonzero β , this is the first guess in an iteration procedure that converged in two iterations for all tested cases.

Initial conditions specify balanced flow above 200 m, decreasing smoothly to zero at the surface. For the case of strong diurnal oscillations of eddy stress and of the pressure gradient, the solutions after a day of integration depend relatively little on initial conditions. By the end of the second day, all solutions become periodic for all

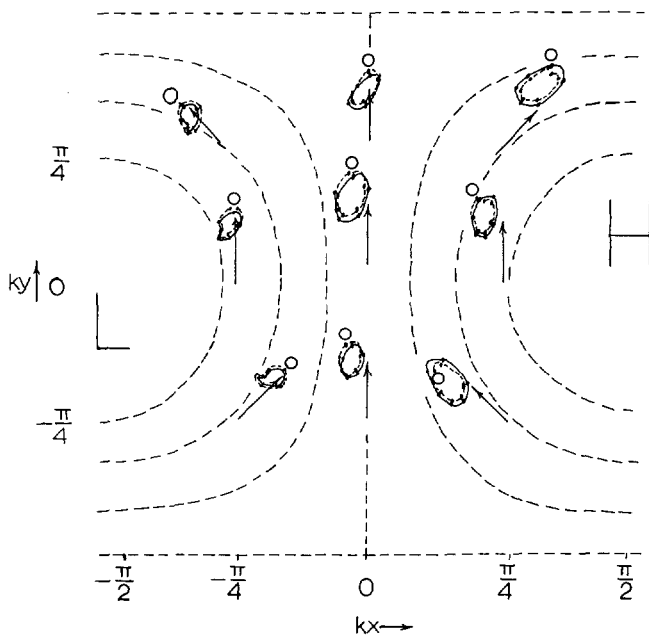


FIGURE 3.—Experiment 1—500-m horizontal winds. Elliptical curves depict time evolution relative to local geostrophic wind (solid arrows). Solid line curves are computed from method described in text, dashed line curves are from Rasch (1973). Hour zero (time of minimum K) is labeled, and subsequent dots follow clockwise at 4-hr intervals.

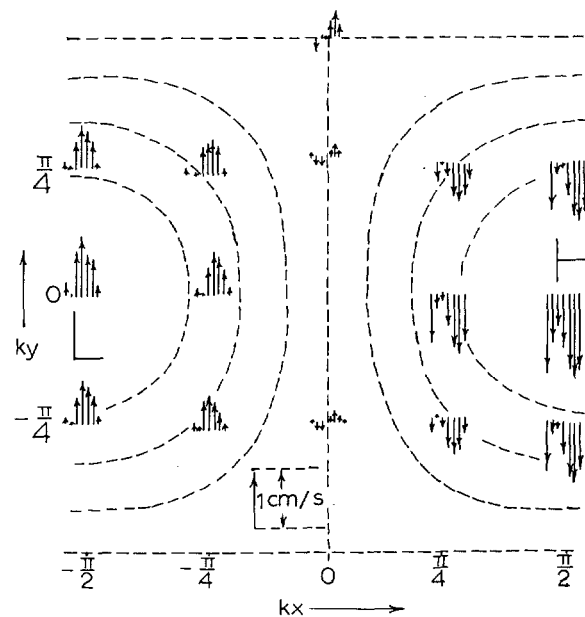


FIGURE 4.—Experiment 1—vertical velocities at the top of the boundary layer. First arrow of every group corresponds to time of minimum K , and subsequent arrows are at 4-hr intervals.

TABLE 1.—Diurnal wind variation as a function of the absolute balanced vorticity

kx	ky	$f+\xi_{\text{balanced}}$	$f+\xi_{\text{balanced}}-\Omega$	Wind variation	
				exp. 1	exp. 3
		(s^{-1})	(s^{-1})	(m/s)	(m/s)
$\pi/4$	$\pm \pi/4$	0.8×10^{-4}	0.07×10^{-4}	9.6	6.5
$\pi/4$	0	$.65 \times 10^{-4}$	$-.09 \times 10^{-4}$	7.1	5.0
$-\pi/4$	$\pm \pi/4$	1.2×10^{-4}	$.37 \times 10^{-4}$	5.2	3.0
$-\pi/4$	0	1.44×10^{-4}	$.61 \times 10^{-4}$	4.9	2.5
0	$\pi/4$	1×10^{-4}	$.2 \times 10^{-4}$	6.9	4.0
0	$-\pi/4$	1×10^{-4}	$.2 \times 10^{-4}$	4.4	2.0
Linear		1×10^{-4}	$.2 \times 10^{-4}$	5.4	2.3

practical purposes, with a single exception that will be discussed later.

Various finite-differencing techniques were tested and compared. The most satisfactory proved to be Crank Nicholson differencing with respect to friction terms and the simplified (second order) Adams Bashforth scheme with respect to the other terms (Gerald 1970). A 20-min time step is used since results obtained with this time step compare very closely with those obtained with a smaller time step. Thirty-five levels resolve the vertical dimension, with the bottom boundary at the roughness height of 1 cm and the top boundary close to 2000 m. Grid spacing is an exponential function of z in the lowest 200 m and constant above that level. A logarithmic transformation of the height variable is used in the lowest 200 m. An integration for 100 hr requires 20 s of UNIVAC 1108 computer time.¹

Programs and finite-difference methods were checked against available steady-state solutions of Benton et al. (1964) and Rogers and Lance (1960). In all cases, the solutions tended to those of the steady-state cases from initially unbalanced states but approached steady state very slowly in instances of cyclonic relative vorticity. For anticyclonic systems, the convergence was much more rapid. To a certain extent, this was also true for approach to periodicity in the case of periodic K and pressure gradient.

¹ Mention of a commercial product does not constitute an endorsement.

Numerical Experiments

Five experiments will be discussed for the idealized cellular pressure field depicted in figures 3–12. This pressure field is represented by

$$\frac{p}{\rho} = \frac{f_0 V}{k} \sin(kx) \cos(ky), \quad (32)$$

with $1/k = 750$ km, $V = 15$ m/s, $f_0 = 10^{-4} s^{-1}$, and $\rho =$ density (constant). The relative geostrophic vorticity,

$$\xi_g = -2Vk \sin(kx) \cos(ky), \quad (33)$$

attains the magnitude of $0.4 \times 10^{-4} s^{-1}$ in each circulation center. In all cases, a latitude of 45° is assumed for each point of the flow field.

Experiment 1 (figs. 3, 4, table 1).

$$K = 8.25 (1 - 0.8 \cos \Omega t) \text{ (m}^2/\text{s)}, \quad (34)$$

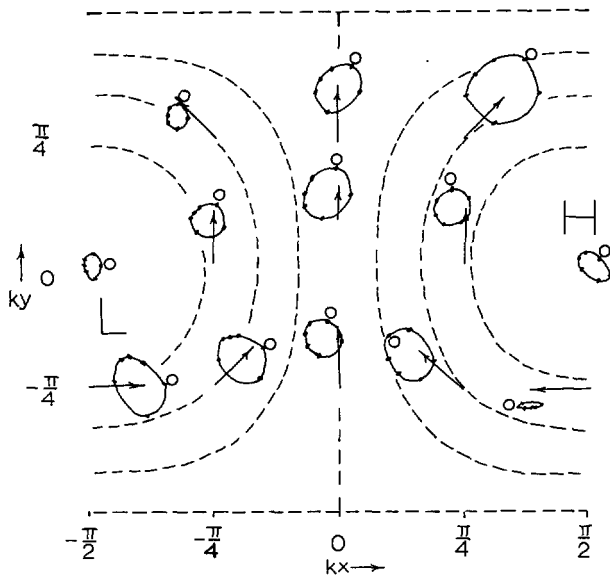


FIGURE 5.—Same as figure 3 for experiment 2.

$$\mathbf{V}_g = \frac{1}{f} \mathbf{K} \times \nabla p, \quad (35)$$

and

$$\beta = 0. \quad (36)$$

This experiment is intended to demonstrate the influence of various large-scale flow structures on the local wind oscillation forced by fluctuations of K alone. Both the mean winds and the diurnal oscillation are stronger around the anticyclone than around the cyclone. This is consistent with the gradient wind equation and with the fact that $f + \xi$ around the high-pressure center is closer to the diurnal forcing frequency ($\Omega = 0.739 \times 10^{-4} \text{ s}^{-1}$) than is $f + \xi$ around the Low. At all plotted points except the central point, the geostrophic winds have magnitude 10.6 m/s. The responses at these points are compared in table 1, which depicts the maximum day to night wind variation at 500 m, the absolute vorticity of the balanced wind, and its difference from the diurnal forcing frequency. In general, stronger response occurs for smaller magnitude of $(f + \xi_{\text{balanced}} - r)$, as expected.

At points $kx = \pi/4$, $ky = \pm \pi/4$, the nocturnal jet is about 70-percent supergeostrophic. These results indicate that the fluctuation of eddy stress may be the main cause of the strongly supergeostrophic nocturnal jets that are sometimes observed. This conclusion will be modified by experiment 3.

Figure 4 depicts vertical velocities at the top of the boundary layer. Sinking occurs over the anticyclone and rising over the cyclone. These vertical velocities are strongest during the afternoon and decrease to practically zero during the night. The magnitude of the vertical motions is stronger over regions of anticyclonic flow than over corresponding portions of cyclonic flow. This is consistent with steady-state results of Benton et al. (1964) and Rogers and Lance (1960), but inconsistent with

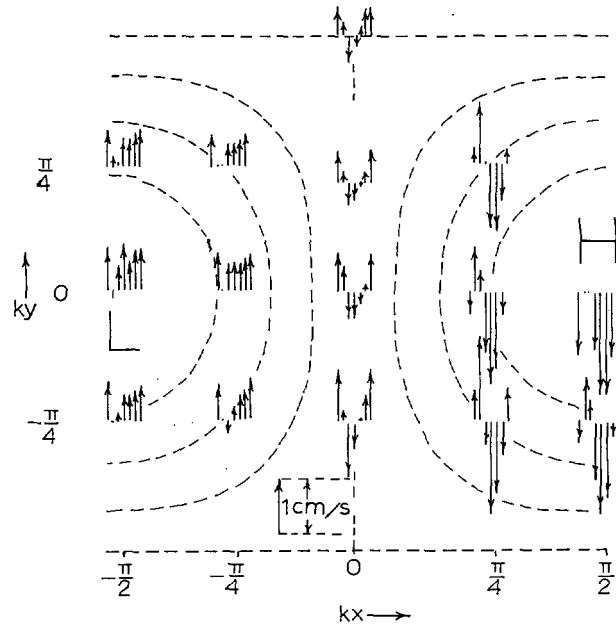


FIGURE 6.—Same as figure 4 for experiment 2.

the steady-state results of Mak (1972). The discrepancy with the latter probably arises from the prespecification of K in the present work, while K was determined as a function of vertical wind shears by Mak.

In another approach to the problem, Rasch (1973) has expanded solutions in the Rossby number. This method has certain limitations, but second derivatives of the flow field are not excluded as in the present approach. Thus, differences between the results of the present approach and the Ro expansion (dashed curves, fig. 3) in experiment 1, might indicate the importance of higher derivatives of the flow field.

All comments made with regard to the dependence of the response on the values of $f + \xi_{\text{balanced}} - \Omega$ hold qualitatively for the Ro expansion solutions. The solutions expanded in the Rossby number require more time to acquire periodicity. However, at the points of greatest dissimilarity (the northwest and southwest quadrants of the high-pressure cell during early morning hours), the disparity between solutions is only about 1 m/s, and the wind in both cases is still 6–7 m/s stronger than the geostrophic wind.

While the solutions agree fairly well up to 500 m, the results above about 1000 m are in poor agreement, and vertical velocities above 2000 m are in total disagreement. The expansion in Ro is apparently not uniformly valid, since, at order Ro^n , functions with factors $z^n e^{-Az} [\text{Re}(A) > 0]$ appear. The solution is not of the boundary-layer type for large order and great heights but, as in similar problems, could be reasonable for nondimensional height not much greater than one. With some caution, then, it might be concluded that up to about 500 m the neglect of higher order horizontal derivatives might not be a critical simplification for the pressure pattern under consideration.

Experiment 2 (figs. 5, 6).

$$K = 8.25 (1 - 0.8 \cos \Omega t) \quad (\text{m}^2/\text{s}), \quad (37)$$

$$\mathbf{V}_g = \frac{1}{\rho f} \mathbf{K} \times \nabla P - \mathbf{j} 4e^{-z/800} \cos [\Omega(t-3 \text{ hr})] \text{ (m/s)}, \quad (38)$$

$$V_{gz} = 10^{-5} e^{-z/800} \cos [\Omega(t-3 \text{ hr})] + \frac{1}{\rho f} \frac{\partial^2 p}{\partial x^2} \text{ (s}^{-1}\text{)}, \quad (39)$$

and

$$\beta = 0. \quad (40)$$

This specification of geostrophic flow models the effect of a terrain sloping gently upward from east to west. The v_{gz} term models a broad valley curvature effect. The phasing and magnitude are representative of terrain around Kansas City.

Neglecting small terrain curvature terms, the equations derived earlier in this section can be shown to apply in a coordinate system with the z axis perpendicular to the local terrain, the y axis pointing northward, and the x axis pointing eastward and locally parallel to the terrain slope.

The pressure gradient oscillation substantially amplifies the wind oscillation. The maximum wind is in the southwesterly flow of the anticyclone where the nocturnal jet is 80 percent stronger than the geostrophic wind. Quite large oscillations also exist in the southeastern quadrant of the low-pressure cell, but here maxima are only about 30 percent supergeostrophic.

The vertical motion field (fig. 6) is of particular interest in this case. Over most of the anticyclone and over the southerly irrotational flow, rising motion can be seen from about 6 hr before the time of minimum eddy viscosity to about 6 hr after this time. The rest of the time, sinking is dominant. Thus, the terrain configuration around Kansas City, Mo., would induce convergence and rising motion at night and divergence and sinking motion during the day for a large portion of this southerly flow. This is consistent with the frequent occurrence of nocturnal thunderstorms around Kansas City.

This result is due to the drainage convergence of air into a broad valley at night and daytime upslope divergence, modeled through the diurnal variation of v_{gz} . Its possible relation to nocturnal thunderstorms over portions of the Great Plains has been pointed out by Means (1952) and Pitchford and London (1962). It is notable that within a fairly strong anticyclonic system the effect is sufficiently pronounced to produce rising motion on the order of 1 cm/s each night and sinking of stronger magnitude during the day. A major limitation to quantitative estimates of this boundary-layer convergence is the very arbitrary specification of friction. It will be shown that a more acceptable formulation of eddy viscosity leads to even larger nocturnal rising and afternoon sinking.

The next three experiments include a more consistent formulation for eddy viscosity. The results of models of this type are not extremely sensitive to the magnitude of K , but do depend significantly on the variation of K with height, particularly at low levels. While appropriate values of K above about 50 m are only very vaguely known, much more is understood about its variation at

lower levels for both stable and unstable stratification. The appendix describes a formulation that at low levels is consistent with available theory and which is used for the next three experiments.

Experiment 3 (figs. 7, 8, table 1). Height dependent, time dependent K (see appendix).

$$\mathbf{V}_g = \frac{1}{\rho f} \mathbf{K} \times \nabla p, \quad (41)$$

and

$$\beta = 0. \quad (42)$$

Results indicate diurnal oscillations only 50 to 70 percent as strong as those for the case when K is constant in height (experiment 1) and the vertical motions have magnitudes only half as strong. Otherwise, results are qualitatively similar to those of experiment 1. The weaker response results from the fact that the cross-isobar angle during the afternoon being smaller in this experiment than with K constant in height. Thus, the afternoon ageostrophic component is weaker, and the nocturnal inertial rotation is much less prominent than in the earlier experiments. From this result, it appears that the diurnal oscillation of eddy stress is not a likely cause of very sizeable low-level jets.

Experiment 4 (figs. 9, 10). Height-dependent, time-dependent K (see appendix).

$$\mathbf{V}_g = \frac{1}{\rho f} \mathbf{K} \times \nabla p - \mathbf{j} 4e^{-z/800} \cos [\Omega(t-3 \text{ hr})] \text{ m/s}, \quad (43)$$

$$v_{gz} = 10^{-5} e^{-z/800} \cos [\Omega(t-3 \text{ hr})] + \frac{1}{\rho f} \frac{\partial^2 p}{\partial x^2}, \quad (44)$$

and

$$\beta = 0. \quad (45)$$

Except for the more realistic K , these specifications are equivalent to conditions of experiment 2. The flow exhibits strong diurnal oscillation and reaches twice geostrophic speeds to the northwest and southwest of the high-pressure center. The vertical motions also have larger amplitude and exhibit marked sinking during the afternoon and rising at night, particularly over the southerly jet axis and in western portions of the anticyclone. In the southwestern quadrant of the anticyclone, w is close to 3 cm/s during the few hours following the time of minimum eddy viscosity, and slightly stronger sinking is indicated around the time of maximum eddy viscosity. An air column extending from the surface to 2000 m would stretch about 600 m at night and compress about 800 m during the daylight hours. This would have a significant destabilizing effect on the boundary layer at night and a stabilizing influence during the afternoon, particularly above about 500 m, where this might dominate opposing radiational effects.

In this case, the magnitude of K averaged over a day and over the depth of the boundary layer is larger than that of experiment 2, yet the frictional damping is apparently less. The reason for this is that the surface stress in the present experiment is only half as large as that in

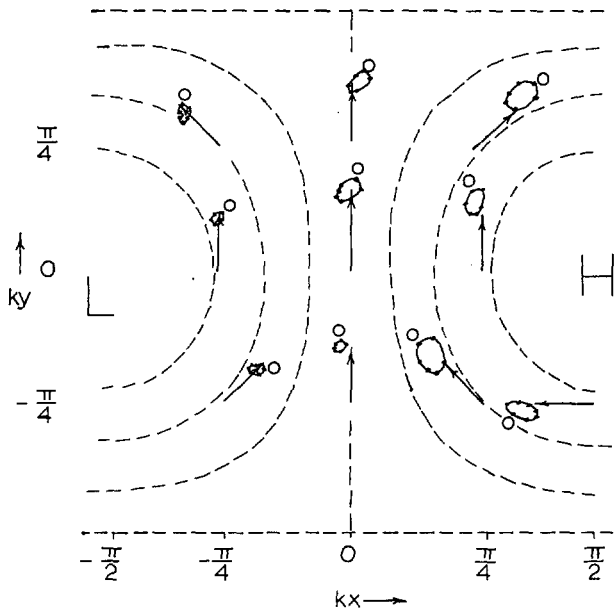


FIGURE 7.—Same as figure 3 for experiment 3.

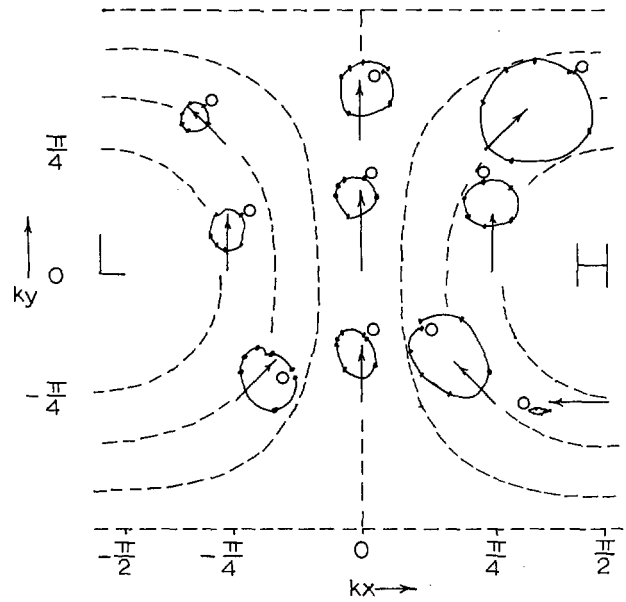


FIGURE 9.—Same as figure 3 for experiment 4.

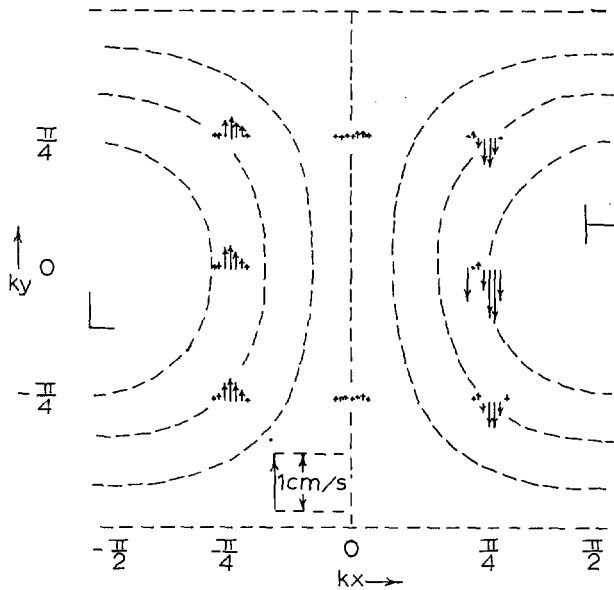


FIGURE 8.—Same as figure 4 for experiment 3.

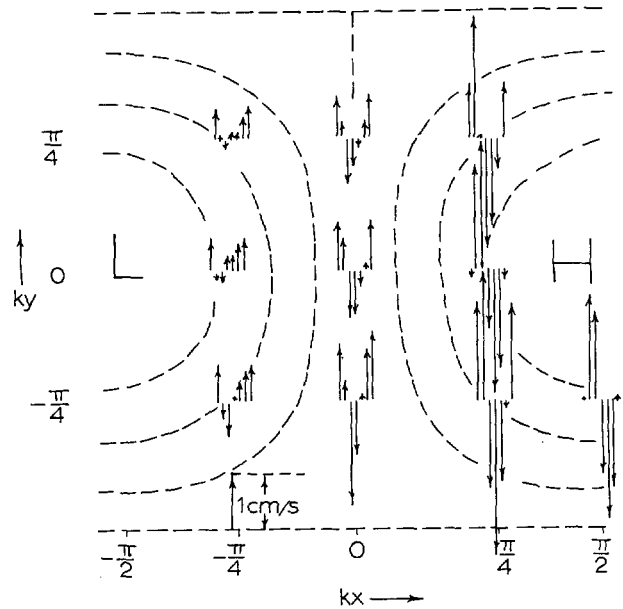


FIGURE 10.—Same as figure 4 for experiment 4.

experiment 2. This indicates that the vertical profile of K has more bearing on the wind than its average magnitude and that the results do not depend too sensitively on the magnitude of K at higher levels, so long as the low-level specification is reasonable.

Experiment 5 (figs. 11, 12). Same as experiment 4 but with $\beta = 1.5 \times 10^{-11} \text{ m}^{-1} \text{ s}^{-1}$. This experiment illustrates the effect of the earth's curvature. The results are qualitatively similar to those of the last subsection, but the diurnal oscillations are about 10–20 percent larger. Part of this may be explained by the fact that in southerly flow the β effect tends to decrease the absolute vorticity at fixed points so that it becomes closer to the critical value over most of the flow field. The β effect also tends

to change the deformation of the balance wind so that for southerly flow a streamwise deceleration and lateral spreading is accentuated. This sort of deformation pattern apparently favors a larger diurnal oscillation. (in fig. 3 and table 1, compare point $kx=0, ky=+\pi/4$ with $kx=0, ky=-\pi/4$.)

At the point $kx=0, ky=\pi/4$, no periodic solution exists. The reason for this is probably related to the simplifying assumption that local gradients exist to infinite distance. At point $kx=0, ky=\pi/4$, this models a point downstream of an infinite velocity at infinite distance. This assumption has been questioned in the similarity solutions without β or time dependent K (Greenspan 1968), and we are still investigating this strongly limiting feature of the solutions.

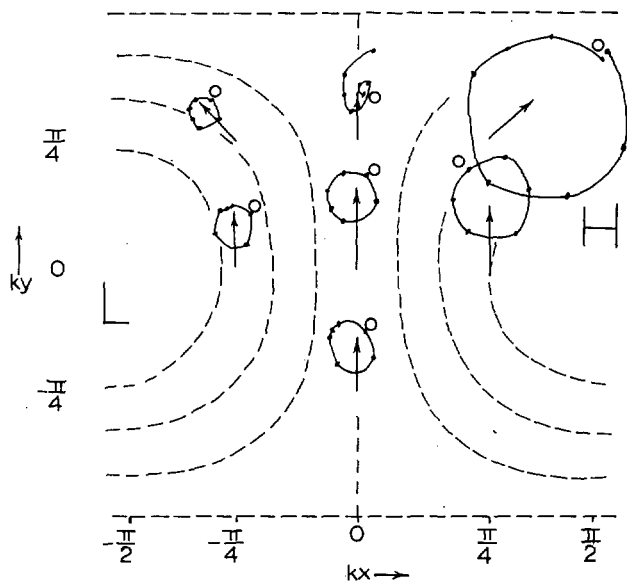


FIGURE 11.—Same as figure 3 for experiment 5.

5. CONCLUDING COMMENTS

It may be summarized that the horizontally nonuniform, nonsteady aspects of boundary layers can be quite critical in the presence of forcings with frequency close to f . The steady-state, linearized, boundary-layer model predictions are not only quantitatively different but can be qualitatively wrong. An example would be the prediction of boundary-layer motion around moderate anticyclones, as in experiment 4, over very slight terrain slopes (1/500). Applying steady-state linear theory, one would obtain a horizontal wind at 500 m that would be close to geostrophic, and the flow would be characterized by divergence and sinking motion. The present results indicate that for a substantial portion of the oscillation (much of the night) the wind can easily be more than 50 percent stronger than geostrophic and that marked convergence and rising motion may occur.

The correspondence of the solutions to Great Plains observations is good. Strongly supergeostrophic nocturnal jets and boundary-layer convergence are predicted in regions where the nighttime jet and thunderstorms are both common. The velocities of the jet drop much more sharply to the left of the jet than to the right. This results in larger cyclonic vorticity than anticyclonic vorticity on the flanks of the jet in agreement with observations of Bonner et al. (1968). The model predicts the strongest southerly jets in the western portions of anticyclonic circulation. The presence of a broad southerly flow around the western flank of the Bermuda anticyclone has been cited as a requisite for a strong jet (Bonner 1968, Wexler 1961).

It appears that the greatest single contributing factor to the nocturnal jet, and certainly to the nocturnal convergence pattern, is the Great Plains topography. The eddy stress oscillation is apparently of lesser importance.

There are several weaknesses in the present approach. First, the formulation of eddy stresses is rather arbitrary.

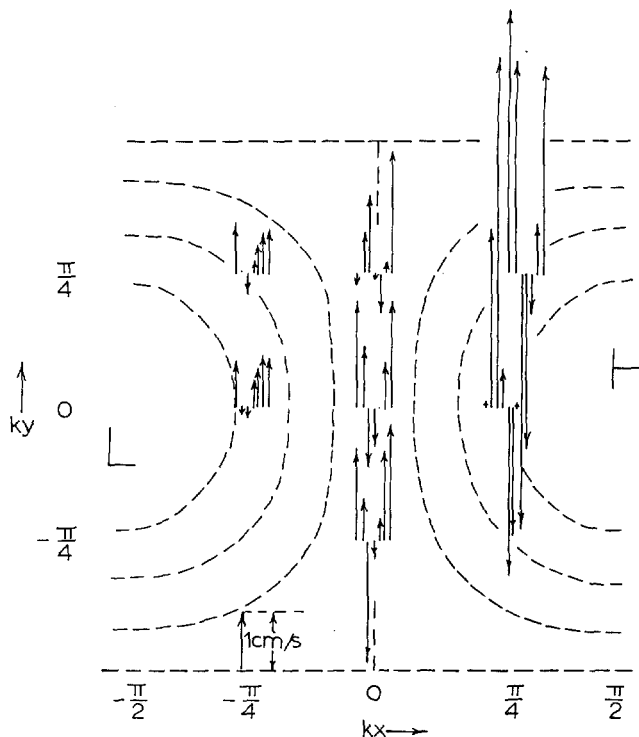


FIGURE 12.—Same as figure 4 for experiment 5.

The results are particularly sensitive to specification of K within the lowest few tens of meters. Fortunately, this is the region where K can be formulated most realistically. The dependence on the values of K at higher levels is not nearly as sensitive, but it is very difficult to determine appropriate numbers, especially for unstable stratification.

A second weak point of the model is the neglect of second horizontal derivatives of the flow field. The quantitative differences between experiments 4 and 5 are notable, indicating the importance of the β effect. Relative vorticity advectations are often as important as the β effect and cannot be reproduced by the present approach. Experiment 1 indicates that higher order derivatives in the flow field are not critical in the particular flow field studied, but they are likely to be of greater importance for propagating pressure patterns.

Another simplification is the implicit assumption of neutral stratification. A more realistic stratification would be somewhat stable on a daily average and would probably tend to reduce the amplitude of the response.

APPENDIX

The specification of K is made so that under conditions of steady state, neutral stratification, and horizontal homogeneity, the results are consistent with accepted surface layer theory. The effect of stability fluctuation is incorporated by a specified variation of the Monin-Obukhov scale length L ; that is,

$$L = -\frac{u_*^3}{\frac{kg}{T} w' \theta'} \quad (46)$$

where

$$T = \text{mean temperature,} \quad (47)$$

$$u_* = \text{friction velocity,} \quad (48)$$

$$k = \text{The von Kármán constant,} \quad (49)$$

$$g = \text{gravity} \quad (50)$$

and

$$\overline{w'\theta'} = \text{the vertical "heat" flux.} \quad (51)$$

A dimensional analysis for the steady-state surface boundary layer indicates that

$$\frac{kz}{u_*} \frac{\partial \bar{u}}{\partial z} = \phi \left(\frac{z}{L} \right) \quad (52)$$

where ϕ is a universal function to be determined from observation. (See, e.g., Plate 1971, pp. 79–83.) Under unstable conditions, ϕ of the form

$$\phi = \left(1 - 15 \frac{z}{L} \right)^{-1/4} \quad (L < 0) \quad (53)$$

fits data well, while under stable conditions

$$\phi = 1 + 4.7 \frac{z}{L} \quad (L > 0) \quad (54)$$

fits data well.

If the eddy stress is specified by an eddy viscosity formulation, then

$$u_*^2 = K \frac{\partial \bar{u}}{\partial z} \quad (55)$$

at low levels; using this in eq (52) gives

$$K = \frac{u_* k z}{\phi \left(\frac{z}{L} \right)} \quad (56)$$

for the surface boundary layer.

In this study, K is specified so that it effectively has the form of eq (56) through the lowest 20 m. At higher levels, this is modified because stratification changes with height and because constant-flux assumptions are reasonable only in a thin surface layer. In the final specification,

$$K = \frac{u_* k z}{(Az^2 + 1) \phi \left(\frac{z}{L} \right)} \quad (57)$$

with

$$A = \{ 1 + 0.9 [\sin(\cos \Omega t)] \sqrt{|\cos \Omega t|} \} 0.0001 \text{ m}^{-2} \quad (58)$$

for unstable stratification,

$$A = 0 \text{ for stable stratification,} \quad (59)$$

$$L = \begin{cases} \frac{4 a u_*^3}{0.013 \cos \Omega t} \text{ m} \\ \text{or 300 m, whichever is smaller,} \end{cases}$$

$$a = \begin{cases} 1 \text{ for unstable stratification} \\ 2 \text{ for stable stratification,} \end{cases}$$

and

$$u_* = 0.037 |\mathbf{V}_g|. \quad (60)$$

The value u_* might well depend on stability, although there is some discussion on this point (Swinbank 1967). We specify it to be consistent with a neutral model and data presented by Blackadar (1962) for a surface Rossby number between 10^6 and 10^7 . For a 10 m/s wind, L ranges over (–300, –16) and (32, 600) for unstable and stable conditions, respectively. These magnitudes are consistent with data presented by Monin and Obukhov (1954).

The arbitrary specifications of eq (57)–(59) are designed to produce a K with maximum amplitude at 500 m during the midafternoon and at somewhat lower levels during the rest of the unstable hours in the model. During the night, K approaches a constant value asymptotically with height. Although K is a function of position through u_* (and $|\mathbf{V}_g|$), it is treated as locally constant at each point of integration.

ACKNOWLEDGMENTS

This work was supported by NSF Atmospheric Sciences Section Grant GA-28277. We wish also to acknowledge the valuable guidance and encouragement of W. D. Bonner and M. G. Wurtele in the early stages of the research.

REFERENCES

- Allen, Stuart, Commonwealth Bureau of Meteorology, Melbourne, Victoria, Australia, 1971 (personal communication).
- Altinger, Maria-Louisa, Departamento de Meteorologia, Facultad de Ciencias Exactas y Naturales, Universidad de Buenos Aires, Argentina, 1972 (personal communication).
- Benton, George S., Lipps, Frank B., and Tuann, Shih-Yu, "The Structure of the Ekman Layer for Geostrophic Flows With Lateral Shear," *Tellus*, Vol. 16, No. 2, Stockholm, Sweden, May 1964, pp. 186–199.
- Blackadar, Alfred K., "Boundary Layer Wind Maxima and Their Significance for the Growth of Nocturnal Inversions," *Bulletin of the American Meteorological Society*, Vol. 38, No. 5, May 1957, pp. 283–290.
- Blackadar, Alfred K., "The Vertical Distribution of Wind and Turbulent Exchange in a Neutral Atmosphere," *Journal of Geophysical Research*, Vol. 67, No. 8, July 1962, pp. 3095–3102.
- Bonner, William D., "Statistical and Kinematical Properties of the Low Level Jet Stream," *Satellite and Mesometeorology Research Project Paper 38*, University of Chicago, Ill., Jan. 1965, 54 pp.
- Bonner, William D., Esbensen, Steven, and Greenberg, Robert, "Kinematics of the Low-Level Jet," *Journal of Applied Meteorology*, Vol. 7, No. 3, June 1968, pp. 339–347.
- Bonner, William D., and Paegle, Jan, "Diurnal Variations in Boundary Layer Winds Over the South-Central United States in Summer," *Monthly Weather Review*, Vol. 98, No. 10, Oct. 1970, pp. 735–744.
- Buajitti, K. and Blackadar, A., "Theoretical Studies of Diurnal Wind Variations in the Planetary Boundary Layer," *Quarterly Journal of the Royal Meteorological Society*, Vol. 83, No. 353, London, England, Oct. 1957, pp. 486–500.
- Farquharson, J. S., "The Diurnal Variation of Wind Over Tropical Africa," *Quarterly Journal of the Royal Meteorological Society*, Vol. 65, No. 280, London, England, Apr. 1939, pp. 165–183.
- Gerald, C. F., *Applied Numerical Analysis*, Addison Wesley Publishing Co. Inc., New York, N. Y., 1970, 340 pp.
- Greenspan, H. P., *The Theory of Rotating Fluids*, Cambridge University Press, England, 1968, 327 pp.
- Holton, James R., "The Diurnal Boundary Layer Wind Oscillation Above Sloping Terrain," *Tellus*, Vol. 19, No. 2, Stockholm, Sweden, 1967, pp. 199–205.
- Kendrew, W. G., *Climatology*, Oxford University Press, London, England, 1957, 400 pp.

- Krishna, K., "A Numerical Study of the Diurnal Variation of Meteorological Parameters in the Planetary Boundary Layer: I. Diurnal Variations of Winds," *Monthly Weather Review*, Vol. 96, No. 5, May 1968, pp. 269-276.
- Mak, Man-Kin, "Steady, Neutral Planetary Boundary Layer Forced by a Horizontally Non-Uniform Flow," *Journal of the Atmospheric Sciences*, Vol. 29, No. 4, May 1972, pp. 707-717.
- Means, Lynn L., "On Thunderstorm Forecasting in the Central United States," *Monthly Weather Review*, Vol. 80, No. 10, Oct. 1952, pp. 165-189.
- Monin, A. S., and Obukhov, A. M., "Basic Regularity in Turbulent Mixing in the Surface Layer of the Atmosphere," *Works of the Geophysical Institute, USSR Academy of Science*, No. 24, (151) Moscow, 1954, pp. 163-187.
- Novozhilov, N., "Tropospheric Meso Currents," *Bulletin of the Academy of Sciences, USSR, Geophysics Series*, Vol. 2, Moscow, Feb. 1961, pp. 334-336.
- Ooyama, Katsuyuki, "A Study of Diurnal Variations of Wind Caused by Periodic Variation of Eddy Viscosity," *Final Report*, Contract No. AF(604)-1368, College of Engineering, New York University, Bronx, N. Y., May 1957, pp. 80-135.
- Paegle, Jan, "Studies of Diurnally Periodic Boundary Layer Winds," *Technical Report*, NSF Grant GA-698, Department of Meteorology, University of California, Los Angeles, 1970, 69 pp.
- Pitchford, Kenneth L., and London, Julius, "The Low-Level Jet as Related to Nocturnal Thunderstorms Over Midwest United States," *Journal of Applied Meteorology*, Vol. 1, No. 1, Mar. 1962, pp. 43-47.
- Plate, Erich J., *Aerodynamic Characteristics of Atmospheric Boundary Layers*, USAEC Division of Technical Information Extension, Oakridge, Tenn., May 1971, 190 pp.
- Rasch, Glenn E., "Rossby Number Expansion of the Planetary Boundary Layer Equations," Masters thesis, Department of Meteorology, University of Utah, Salt Lake City, 1973, 81 pp.
- Rogers, M. H., and Lance, G. N., "The Rotationally Symmetric Flow of a Viscous Fluid in the Presence of an Infinite Rotating Disk," *Journal of Fluid Mechanics*, Vol. 7, Part 4, Apr. 1960, pp. 617-631.
- Sangster, Wayne E., "Diurnal Surface Geostrophic Wind Variations Over the Great Plains," ESSA, Central Region, *Technical Memorandum* 13, Mar. 1967, Kansas City, Mo. 16 pp.
- Swinbank, W. C., "A Dimensional Analysis of the Constant Flux Layer," CSIRO Division of Meteorological Physics, Aspendale, Australia, 1967, 13 pp. (Unpublished manuscript.)
- Wexler, Harry, "A Boundary Layer Interpretation of the Low-Level Jet," *Tellus*, Vol. 13, No. 3, Stockholm, Sweden, Aug. 1961, pp. 368-378.

[Received April 27, 1973; revised August 17, 1973]